

Structure and ionization energies of some analogues of iron-only hydrogenases studied by density functional theory methods

Prabha Jayapal, Mahesh Sundararajan, Ian H. Hillier^{*}, Neil A. Burton

School of Chemistry, University of Manchester, Manchester M13 9PL, UK

Received 20 January 2006; received in revised form 15 March 2006; accepted 18 April 2006

Available online 26 April 2006

Abstract

Density functional theory calculations using both the B3LYP and BP86 functional in conjunction with a medium and large size basis set have been used to predict the structures and ionization energies of 12 models of iron-only hydrogenases. Although the structural predictions do not allow a clear discrimination between the different computational models, these models do yield significantly different adiabatic and vertical ionization energies. The closest agreement with experiment is given by the BP86 functional and the large all-electron basis. At this level of theory the adiabatic ionization energies are very close to experiment, but the vertical values are uniformly too small, leading to an underestimation of the reorganization energies. The calculations also suggest that measured ionization energies may help in identifying both the bridge-head group and whether CO bridging takes place upon ionization.

© 2006 Elsevier B.V. All rights reserved.

Keywords: Density functional theory; Iron-only hydrogenases; Photoelectron spectroscopy; Ionization energy

1. Introduction

An understanding of the structure–function relationships in metalloproteins is now sought through a combination of structural, spectroscopic and modelling techniques, which can involve both the actual protein and synthetic models of the active site [1]. Electron transfer is often central to the mode of action of many such proteins and for this reason experiments and modelling studies have focused on understanding the redox properties of the metal centre [2]. This has led to a resurgence in the use of photoelectron spectroscopy (PES) to study the ionization process [3]. This technique can yield both the vertical and adiabatic electron detachment energies (VDE, ADE), the difference between these quantities being the reorganization energy λ_{oxi} , a quantity central to the Marcus theory of electron transfer, which can lead to predictions of the rate of the actual redox reaction [4–6]. Although PES has traditionally been used in

the study of neutral transition metal complexes, the use of an electrospray ionization (ESI) technique allows the PES of charged species to be studied, and has greatly expanded the range of models of metalloproteins which can be studied by this technique [5,7]. Other workers have used PES to study the electronic structure of active site analogues of a number of proteins, whilst we and others have used these experimental data to assess the appropriate functional and basis set for the investigation of iron sulfur proteins [8–11].

Hydrogenases are an important class of metalloprotein which catalyze the reversible activation of molecular hydrogen



and may thus be used in the future as fuel cells [12]. One such group, the all-iron hydrogenases, involve a di-iron cluster linked by a cysteine thiolate to a [4Fe4S] cluster to give the so-called H-cluster [13] (Fig. 1). The redox reaction involving hydrogen takes place at the di-iron cluster, with the [4Fe4S] cluster providing an electron source and sink. There are many questions concerning the actual

^{*} Corresponding author. Tel.: +44 161 275 4686; fax: +44 161 275 4734.
E-mail address: Ian.Hillier@manchester.ac.uk (I.H. Hillier).

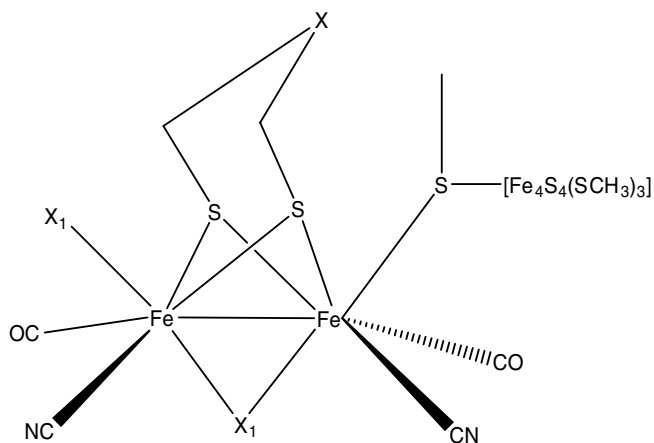


Fig. 1. Active site structure of Fe-only hydrogenase. The bridge-head atom X can be N, O, C; X₁ can be CO or H₂ or vacant.

reaction taking place at the di-iron centre, in particular the various oxidation states of the two iron atoms and the actual identity of the bridge-head atom, suggested to be carbon, nitrogen or oxygen [14,15]. In an effort to elucidate the structure and function of the di-iron and [4Fe4S] centres, many synthetic models have been prepared [16–21]. Very recently, Tard et al. [22] synthesized and characterized the H cluster in solution, which is very similar to the active site of the enzyme (CN is absent in the synthetic cluster) but its crystal structure is yet to be determined.

Yang et al. have used the ESI-PES technique to measure the ionization energies of a series of Fe(I)–Fe(I) complexes which may be models of the di-iron subsite [23]. The structures of a number of these, and related complexes, have also been determined [16,17]. On the modelling side, the size and electronic complexity of these polynuclear metal complexes has meant that *ab initio* methods, which include

a high level of explicit electron correlation, cannot be used to study them. As in many other chemical areas where electronic structure methods are used, the technique most commonly used to model hydrogenases is density functional theory (DFT) [14,15,24,25]. However, it is precisely in the area of transition metal complexes, where a manifold of closely spaced states of different spin multiplicity is often found, that DFT needs to be used judiciously, since the popular hybrid functionals such as B3LYP contain some Hartree–Fock exchange, which can affect the relative energies of such states. Indeed, there is some controversy as to the most appropriate functional to use in the study of metal containing hydrogenases [24]. The lack of high level *ab initio* calculations to judge the accuracy of different functionals means that there is a need for experimental data of model systems, both structural and energetic, to compare with the predictions from different functionals. In this paper, we compare such experimental data for a number of model compounds of the di-iron subsite with predictions using two sets of functionals and basis sets.

2. Computational details

We have studied both the geometric structures and ionization energies of 10 synthetic model compounds (I–V and VIII–XII) and two analogous clusters (VI and VII) corresponding to the enzyme active site, shown in Figs. 2 and 3. The model compounds have a number of structural features in common with the enzyme, in particular two bridging sulphurs and CO, or both CO and CN ligands, bound to the iron atoms. Five of the models (I–V) studied here have been synthesized by Razavet et al. [16,17,24] to both mimic the active site of the Fe-only hydrogenase and to help explain the cyanation mechanism. Some of these species have also been structurally and spectroscopically

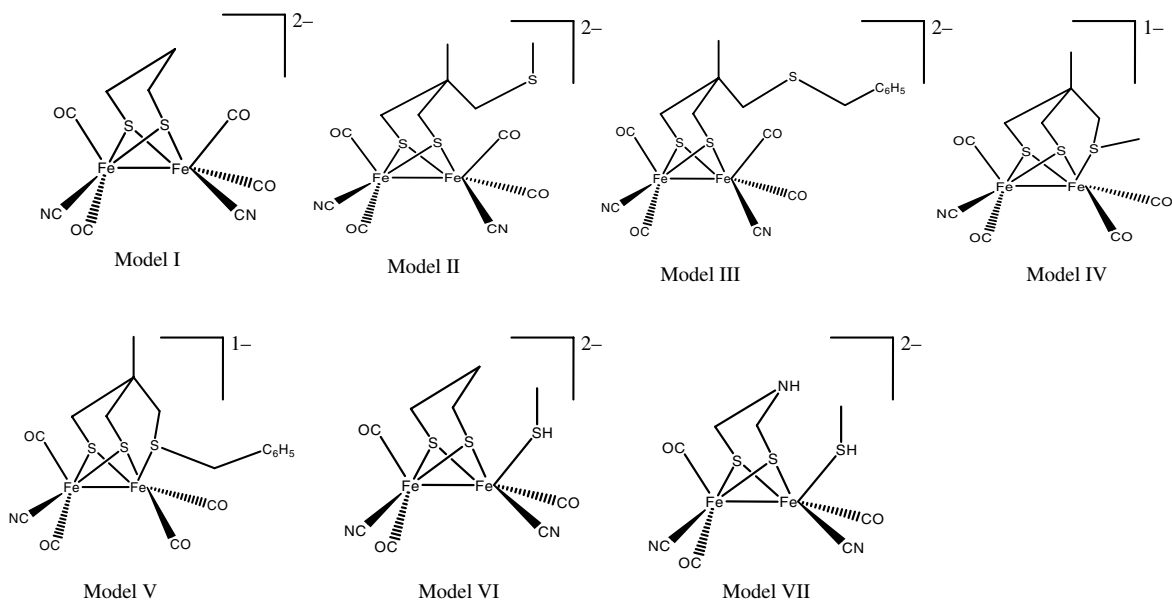


Fig. 2. Analogues (I–VII) of Fe-only hydrogenases.

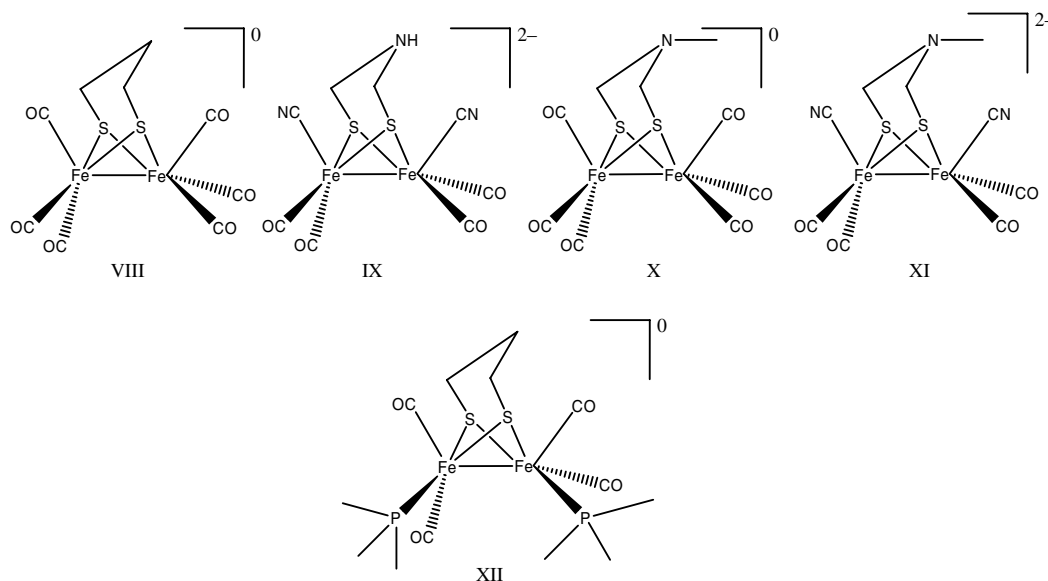


Fig. 3. Analogues (VIII–XII) of Fe-only hydrogenases.

characterized, and studied by DFT methods. In particular, the PES of compounds I–V have been measured by Yang et al. [23]. There are crystal structure data for two of these compounds (I and IV), and for the remaining three in which the CN ligands have been replaced by CO ligands. Clusters VI and VII were prepared from the structure of *Desulfovibrio vulgaris* (PDB code: 1HFE), to include two possibilities for the bridge-head group (CH₂ or NH) [13]. We have also studied a range of synthetic molecules which are analogues of the iron only hydrogenases (VIII–XII) [18,20,26,27]. This set of molecules differs from the previous group (I–VII) by the lack of a third sulfur atom. They differ in their actual charge, the bridge-head group and in the number of CN ligands, with (XII) having two trimethyl phosphine groups in place of the enzymatic cyanides. Structural data are available for these five molecules, but there is a lack of ionization energy data. The two neutral species (VIII and X) differ only in the bridge-head (CH₂ and NMe respectively), the two doubly charged species, (IX and XI) having NH and NMe bridge-heads. These models (VIII and X) are related to IX and XI via cyanation. Model XII has two neutral phosphorous ligands to mimic the anionic cyanides as discussed by Zhao et al. [27]. Recently, a similar model has been synthesized having a hydride ion bridging the two iron atoms [28].

In the calculations of these 12 molecules, we have employed two of the most common functionals (B3LYP and BP86) [29,30], B3LYP having 20% Hartree–Fock exchange whilst BP86 has none. We use two different basis sets (BS1 – LANL2DZ* basis for Fe and S, D95V* basis for CO and CN, 3-21G basis for other atoms; BS2 – 6-311++G** basis for all atoms) [31,32]. For BS1, which involves a pseudopotential on the Fe and S atoms, the total number of basis functions is in the range 297–411, and for the larger all electron basis, BS2, this number is up to 846. The basis, BS1, was chosen by Cao and Hall to study the

reaction mechanism of Fe-only hydrogenase models by monitoring the vibrational frequencies of the CO and CN ligands of the species involved in the reaction [15]. All calculations were performed using GAUSSIAN 03 [33]. The initial structures for the synthetic models were taken from the Cambridge structural database [34].

3. Computational results

3.1. Synthetic cluster results

We first discuss the structures and ionization energies of the model compounds I–V shown in Tables 1 and 2. We see that both functionals and both basis sets generally predict the Fe–Fe and Fe–ligand distances to within 0.1 Å. The calculated structures using the two functionals differ mainly in the changes in the Fe–Fe distances upon ionization. We see there is no systematic way in which these lengths change with the different functionals and basis sets. Furthermore, both functionals predict CO and CN vibrational frequencies consistent with experiment [15,25].

However, we find the predictions to be quantitatively different as far as the ionization energies are concerned. For both basis sets, the VDE and ADE values are systematically smaller for the B3LYP, compared to the BP86 functional (Tables 1 and 2). Indeed, for the doubly charged anions, the B3LYP functional gives a negative VDE and ADE in most cases. The difference in the ionization energies given by the two functionals is fairly constant at 0.3–0.4 eV for both basis sets, reflecting the localized (Fe 3d) nature of the ionization in all the compounds, with the absolute values being ~0.2 eV greater for the larger basis (BS2) (Table 2). It is the BP86 functional, combined with the larger basis set (BS2) which gives the best agreement with the experimental ionization energies. The VDE values are uniformly too small by ~0.3 eV, although the ADE

Table 1
Calculated Fe–X bond lengths (Å) and electron detachment energies (eV) of Fe-only hydrogenase models (I–V) using basis B1

Models	X	Fe–X bond length					Energies			
		Reduced			Oxidized		Experiment ^b	B3LYP/BS1	BP86/BS1	
		X-ray ^a	B3LYP/BS1	BP86/BS1	B3LYP/BS1	BP86/BS1				
I	Fe	2.52	2.56	2.59	2.68	2.66	VDE	0.67(10)	–0.17	0.15
	S ^c	2.27–2.29	2.33–2.36	2.31–2.33	2.32–2.38	2.29–2.37	ADE	0.15(10)	–0.44	–0.07
	C _{CO}	1.71–1.79	1.74–1.75	1.74	1.76–1.78	1.73–1.75	λ_{oxi}	0.52	0.27	0.22
	C _{CN}	1.92–1.94	1.92	1.89–1.90	1.90–1.91	1.87–1.88				
II	Fe	2.49	2.59	2.62	2.59	2.56	VDE	0.84(10)	–0.15	0.16
	S ^c	2.25–2.27	2.32–2.36	2.32–2.33	2.29–2.41	2.26–2.39	ADE	0.25(10)	–0.39	–0.02
	C _{CO}	1.79–1.81	1.74–1.76	1.73–1.75	1.75–1.80	1.73–1.77	λ_{oxi}	0.59	0.24	0.18
	C _{CN}	–	1.92	1.89–1.90	1.90–1.91	1.87–1.89				
III	Fe	2.49	2.60	2.62	2.58	2.56	VDE	0.95(10)	–0.08	0.21
	S ^c	2.25–2.27	2.33–2.36	2.31–2.34	2.30–2.41	2.27–2.39	ADE	0.35(10)	–0.34	0.04
	C _{CO}	1.79–1.81	1.74–1.76	1.73–1.75	1.75–1.80	1.73–1.77	λ_{oxi}	0.60	0.26	0.17
	C _{CN}	–	1.92	1.89–1.90	1.90–1.91	1.87–1.89				
IV	Fe	2.54	2.51	2.54	2.67	2.51	VDE	3.9(1)	3.04	3.41
	S ^c	2.24–2.26	2.32–2.34	2.29–2.32	2.31–2.36	2.26–2.36	ADE	3.30(10)	2.78	3.19
	S	2.25	2.27	2.24	2.32	2.25	λ_{oxi}	0.60	0.26	0.22
	C _{CO}	1.75–1.77	1.75–1.77	1.73–1.75	1.77–1.80	1.76–1.77				
	C _{CN}	1.94	1.92	1.90	1.90	1.86				
V	Fe	2.50	2.51	2.54	2.65	2.50	VDE	3.86(8)	3.03	3.41
	S ^c	2.25–2.26	2.31–2.34	2.29–2.32	2.31–2.37	2.30–2.36	ADE	3.30(8)	2.77	3.18
	S	2.23	2.27	2.23	2.32	2.25	λ_{oxi}	0.56	0.26	0.23
	C _{CO}	1.76–1.78	1.75–1.77	1.74–1.75	1.77–1.80	1.76–1.77				
	C _{CN}	–	1.92	1.89	1.90	1.86				

^a X-ray values are for Fe(I)–Fe(I) species.

^b Values are taken from [23].

^c Denotes bridging atom.

values are in excellent agreement with experiment. This leads to the computed reorganization energies being smaller than the experimental values by ~ 0.3 eV. We have noted a similar, though smaller underestimation of the reorganization energies in our study of rubredoxin analogues [11].

It is of interest to note that on the basis of FTIR spectra of the oxidized form of model II, it has been suggested that ionization may lead to a CO (on the proximal iron) being bridged with the distal iron, and the sulfur being bound to the proximal iron. Calculation of this latter species (BP86/BS2) leads to an ADE of -0.25 eV which is consistent with electrochemical measurements [17]. However, our calculated ADE ($+0.25$ eV) for model II in which no such rearrangement has taken place, is in excellent agreement with the PES value suggesting the bridged CO species can be ruled out in the gas phase.

3.2. Enzyme active site results

We now describe our predictions of the structures and ionization energies for the two clusters (VI and VII) which are models of the actual enzyme active site (Tables 3 and 4). We find that for both species the Fe–Fe bond length increases when the B3LYP functional is used, but decreases for the BP86 functional. This effect has been previously noted [15,25] for these two functionals, but there are no experimental data to test these different predictions. Our

calculated structures of VI for both the reduced and oxidized states using B3LYP/BS1 are in good agreement with those previously reported by Cao and Hall (species 11 and 18 in [15]), and we also find that the terminal CO in the reduced state becomes bridging in the oxidized species. At the B3LYP/BS1 level there is a lengthening of the Fe–Fe bond during ionization, but this lengthening is smaller with the BS2 basis. There is a corresponding shortening of the Fe–Fe bond upon ionization when both basis sets are used in conjunction with a BP86 functional [25].

As found for the models (I–V), the ionization energies are dependent upon the functional and basis set employed (Tables 3 and 4). We also see that there is a systematic increase in the VDE when the bridge-head group is changed from CH₂ (model VI) to NH (model VII), with the reorganization energy being larger for the latter (Table 3). Although the effect is small, measured ionization energies may possibly be a useful fingerprint for identifying the nature of the bridge-head group. The larger reorganization energies found for the enzyme models (VI and VII), than for the synthetic models (I–V), probably arise from the bridging nature of CO in the oxidized state.

3.3. [2Fe2S] synthetic cluster results

Due to the success of the BP86 functional combined with the BS2 basis, we have studied these molecules

Table 2
Calculated Fe–X bond lengths (Å) and electron detachment energies (eV) of Fe-only hydrogenase models (I–V) using basis BS2

Models	X	Fe–X bond length					Energies			
		Reduced			Oxidized		Experiment ^b	B3LYP/BS2	BP86/BS2	
		X-ray ^a	B3LYP/BS2	BP86/BS2	B3LYP/BS2	BP86/BS2				
I	Fe	2.52	2.58	2.61	2.70	2.68	VDE	0.67(10)	0.00	0.39
	S ^c	2.27–2.29	2.33–2.35	2.31	2.31–2.37	2.29–2.35	ADE	0.15(10)	–0.25	0.18
	C _{CO}	1.71–1.79	1.76–1.77	1.75	1.78–1.80	1.75–1.78	λ_{oxi}	0.52	0.25	0.21
	C _{CN}	1.92–1.94	1.95	1.92	1.92–1.94	1.89–1.91				
II	Fe	2.49	2.61	2.63	2.61	2.58	VDE	0.84(10)	0.05	0.43
	S ^c	2.25–2.27	2.31–2.35	2.30–2.32	2.29–2.39	2.25–2.37	ADE	0.25(10)	–0.19	0.24
	C _{CO}	1.79–1.81	1.75–1.78	1.74–1.76	1.77–1.82	1.75–1.78	λ_{oxi}	0.59	0.24	0.19
	C _{CN}	–	1.94–1.95	1.92–1.93	1.93–1.94	1.90–1.91				
III	Fe	2.49	2.62	2.64	2.60	2.57	VDE	0.95(10)	0.09	0.48
	S ^c	2.25–2.27	2.31–2.34	2.30–2.33	2.29–2.39	2.26–2.37	ADE	0.35(10)	–0.14	0.30
	C _{CO}	1.79–1.81	1.75–1.78	1.74–1.76	1.77–1.82	1.75–1.78	λ_{oxi}	0.60	0.23	0.18
	C _{CN}	–	1.94–1.95	1.92–1.93	1.93–1.94	1.90–1.91				
IV	Fe	2.54	2.53	2.57	2.71	2.51	VDE	3.9(1)	3.15	3.57
	S ^c	2.24–2.26	2.31–2.34	2.28–2.32	2.30–2.36	2.26–2.34	ADE	3.30(10)	2.90	3.35
	S	2.25	2.29	2.25	2.33	2.26	λ_{oxi}	0.60	0.25	0.22
	C _{CO}	1.75–1.77	1.77–1.79	1.75–1.76	1.78–1.83	1.78–1.79				
V	Fe	2.50	2.53	2.56	2.69	2.51	VDE	3.86(8)	3.15	3.57
	S ^c	2.25–2.26	2.31–2.34	2.28–2.31	2.31–2.36	2.26–2.34	ADE	3.30(8)	2.90	3.36
	S	2.23	2.28	2.24	2.33	2.26	λ_{oxi}	0.56	0.25	0.21
	C _{CO}	1.76–1.78	1.77–1.79	1.75–1.76	1.79–1.82	1.78–1.79				
VI	Fe	2.57	2.53	2.57	2.58	2.55	VDE	–0.93	–0.58	
	S ^d	2.28–2.30	2.36–2.38	2.32–2.34	2.37–2.38	2.33–2.38	ADE	–1.22	–0.87	
	S	2.51	2.30	2.22	2.32	2.29	λ_{oxi}	0.29	0.29	
	C _{CO}	1.71–1.80	1.74–1.75	1.72–1.74	1.77	1.74				
VII	Fe	–	2.54	2.58	2.59	2.52	VDE	–0.83	–0.50	
	S ^d	–	2.36–2.39	2.32–2.34	2.35–2.44	2.32–2.36	ADE	–1.25	–0.85	
	S	–	2.30	2.22	2.30	2.26	λ_{oxi}	0.42	0.35	
	C _{CO}	–	1.74–1.75	1.72–1.74	1.77	1.74				
VIII	Fe	–	2.54	2.58	2.59	2.52	VDE	–0.83	–0.50	
	S ^d	–	2.36–2.39	2.32–2.34	2.35–2.44	2.32–2.36	ADE	–1.25	–0.85	
	S	–	2.30	2.22	2.30	2.26	λ_{oxi}	0.42	0.35	
	C _{CO}	–	1.74–1.75	1.72–1.74	1.77	1.74				
IX	Fe	–	2.54	2.58	2.59	2.52	VDE	–0.83	–0.50	
	S ^d	–	2.36–2.39	2.32–2.34	2.35–2.44	2.32–2.36	ADE	–1.25	–0.85	
	S	–	2.30	2.22	2.30	2.26	λ_{oxi}	0.42	0.35	
	C _{CO}	–	1.74–1.75	1.72–1.74	1.77	1.74				
X	Fe	–	2.54	2.58	2.59	2.52	VDE	–0.83	–0.50	
	S ^d	–	2.36–2.39	2.32–2.34	2.35–2.44	2.32–2.36	ADE	–1.25	–0.85	
	S	–	2.30	2.22	2.30	2.26	λ_{oxi}	0.42	0.35	
	C _{CO}	–	1.74–1.75	1.72–1.74	1.77	1.74				
XI	Fe	–	2.54	2.58	2.59	2.52	VDE	–0.83	–0.50	
	S ^d	–	2.36–2.39	2.32–2.34	2.35–2.44	2.32–2.36	ADE	–1.25	–0.85	
	S	–	2.30	2.22	2.30	2.26	λ_{oxi}	0.42	0.35	
	C _{CO}	–	1.74–1.75	1.72–1.74	1.77	1.74				
XII	Fe	–	2.54	2.58	2.59	2.52	VDE	–0.83	–0.50	
	S ^d	–	2.36–2.39	2.32–2.34	2.35–2.44	2.32–2.36	ADE	–1.25	–0.85	
	S	–	2.30	2.22	2.30	2.26	λ_{oxi}	0.42	0.35	
	C _{CO}	–	1.74–1.75	1.72–1.74	1.77	1.74				

^a X-ray values are for Fe(I)–Fe(I) species.

^b Values are taken from [23].

^c Denotes bridging atom.

Table 3
Calculated Fe–X bond lengths (Å) and electron detachment energies (eV) of two active site models of the Fe-only hydrogenase, using basis BS1

Models	X	Fe–X bond length					Energies		
		Reduced			Oxidized		Experiment ^b	B3LYP/BS1	BP86/BS1
		X-ray ^a	B3LYP/BS1	BP86/BS1	B3LYP/BS1	BP86/BS1			
VI	Fe	2.57	2.53	2.57	2.58	2.55	VDE	–0.93	–0.58
	S ^d	2.28–2.30	2.36–2.38	2.32–2.34	2.37–2.38	2.33–2.38	ADE	–1.22	–0.87
	S	2.51	2.30	2.22	2.32	2.29	λ_{oxi}	0.29	0.29
	C _{CO}	1.71–1.80	1.74–1.75	1.72–1.74	1.77	1.74			
	C _{CO} ^d	–	–	–	1.85 ^b , 2.19 ^c	1.86 ^b , 2.03 ^c			
VII	Fe	–	2.54	2.58	2.59	2.52	VDE	–0.83	–0.50
	S ^d	–	2.36–2.39	2.32–2.34	2.35–2.44	2.32–2.36	ADE	–1.25	–0.85
	S	–	2.30	2.22	2.30	2.26	λ_{oxi}	0.42	0.35
	C _{CO}	–	1.74–1.75	1.72–1.74	1.77	1.74			
	C _{CO} ^d	–	–	–	1.80 ^b , 2.43 ^c	1.83 ^b , 2.16 ^c			
VIII	Fe	–	2.54	2.58	2.59	2.52	VDE	–0.83	–0.50
	S ^d	–	2.36–2.39	2.32–2.34	2.35–2.44	2.32–2.36	ADE	–1.25	–0.85
	S	–	2.30	2.22	2.30	2.26	λ_{oxi}	0.42	0.35
	C _{CO}	–	1.74–1.75	1.72–1.74	1.77	1.74			
	C _{CO} ^d	–	–	–	1.80 ^b , 2.43 ^c	1.83 ^b , 2.16 ^c			
IX	Fe	–	2.54	2.58	2.59	2.52	VDE	–0.83	–0.50
	S ^d	–	2.36–2.39	2.32–2.34	2.35–2.44	2.32–2.36	ADE	–1.25	–0.85
	S	–	2.30	2.22	2.30	2.26	λ_{oxi}	0.42	0.35
	C _{CO}	–	1.74–1.75	1.72–1.74	1.77	1.74			
	C _{CO} ^d	–	–	–	1.80 ^b , 2.43 ^c	1.83 ^b , 2.16 ^c			
X	Fe	–	2.54	2.58	2.59	2.52	VDE	–0.83	–0.50
	S ^d	–	2.36–2.39	2.32–2.34	2.35–2.44	2.32–2.36	ADE	–1.25	–0.85
	S	–	2.30	2.22	2.30	2.26	λ_{oxi}	0.42	0.35
	C _{CO}	–	1.74–1.75	1.72–1.74	1.77	1.74			
	C _{CO} ^d	–	–	–	1.80 ^b , 2.43 ^c	1.83 ^b , 2.16 ^c			
XI	Fe	–	2.54	2.58	2.59	2.52	VDE	–0.83	–0.50
	S ^d	–	2.36–2.39	2.32–2.34	2.35–2.44	2.32–2.36	ADE	–1.25	–0.85
	S	–	2.30	2.22	2.30	2.26	λ_{oxi}	0.42	0.35
	C _{CO}	–	1.74–1.75	1.72–1.74	1.77	1.74			
	C _{CO} ^d	–	–	–	1.80 ^b , 2.43 ^c	1.83 ^b , 2.16 ^c			
XII	Fe	–	2.54	2.58	2.59	2.52	VDE	–0.83	–0.50
	S ^d	–	2.36–2.39	2.32–2.34	2.35–2.44	2.32–2.36	ADE	–1.25	–0.85
	S	–	2.30	2.22	2.30	2.26	λ_{oxi}	0.42	0.35
	C _{CO}	–	1.74–1.75	1.72–1.74	1.77	1.74			
	C _{CO} ^d	–	–	–	1.80 ^b , 2.43 ^c	1.83 ^b , 2.16 ^c			

^a X-ray values are taken from [13] (PDB Code: 1HFE).

^b Distances from distal iron.

^c Distances from proximal iron.

^d Denotes bridging atom.

(VIII–XII) only at this level. Again the structures of these species in their reduced state are accurately predicted (Table 5). For the four models VIII–XI, we predict a lengthening of the Fe–Fe bond upon ionization, whereas for XII the bond length is unchanged, which is presumably associated with the two bulky trimethyl phosphine ligands.

In agreement with the results of Lawrence et al., we find the bond lengths to be slightly overestimated by our calculations [26]. For model VIII, the iron–ligand bond lengths are slightly longer than those of reported by Cao and Hall, probably due to the bigger basis (BS2) [15]. Moving from X to XI, where the latter has two CN ligands instead of CO, a

Table 4
Calculated Fe–X bond lengths (Å) and electron detachment energies (eV) of two active site models of the Fe-only hydrogenase, using basis BS2

Models	X	Fe–X bond length					Energies			
		Reduced			Oxidized					
		X-ray ^a	B3LYP/BS2	BP86/BS2	B3LYP/BS2	BP86/BS2		B3LYP/BS2	BP86/BS2	
VI	Fe	2.57	2.55	2.60	2.58	2.55	VDE	–0.75	–0.32	
	S ^d	2.28–2.30	2.35–2.37	2.30–2.32	2.35–2.37	2.31–2.37	ADE	–1.00	–0.60	
	S	2.51	2.30	2.21	2.32	2.30	λ_{oxi}	0.25	0.28	
	C _{CO}	1.71–1.80	1.75–1.77	1.74–1.75	1.78–1.79	1.75–1.76				
	C _{CO} ^d	–	–	–	1.85 ^b , 2.26 ^c	1.87 ^b , 2.04 ^c				
	C _{CN}	1.85–1.87	1.95	1.92	1.95	1.91				
VII	Fe		2.56	2.61	2.60	2.52	VDE	–0.65	–0.25	
	S ^d		2.34–2.38	2.30–2.33	2.35–2.41	2.31–2.35	ADE	–1.00	–0.56	
	S		2.29	2.21	2.30	2.26	λ_{oxi}	0.35	0.31	
	C _{CO}		1.76–1.77	1.74–1.75	1.78–1.79	1.75–1.76				
	C _{CO} ^d		–	–	1.82 ^b , 2.46 ^c	1.85 ^b , 2.15 ^c				
	C _{CN}		1.95	1.92	1.95–1.97	1.91				

^a X-ray values are taken from [13] (PDB Code: 1HFE).

^b Distances from distal iron.

^c Distances from proximal iron.

^d Denotes bridging atom.

Table 5
Calculated structures (Å) and ionization energies (eV) of models (VIII–XII) of Fe-only hydrogenases using BP86/BS2

Models	X	Fe–X			Energies	
		X-ray ^a	Reduced	Oxidized		
VIII	Fe	2.51	2.54	2.67	VDE	8.20
	S ^d	2.25	2.29–2.30	2.27–2.33	ADE	7.91
	C _{CO}	1.80	1.78–1.79	1.78–1.83	λ_{oxi}	0.29
IX	Fe	2.51	2.60	2.74	VDE	0.45
	S ^d	2.28–2.29	2.31–2.32	2.29–2.31	ADE	0.17
	C _{CO}	1.74–1.76	1.75	1.77	λ_{oxi}	0.28
	C _{CN}	1.94	1.93	1.89		
X	Fe	2.49	2.54	2.61	VDE	7.62
	S ^d	2.26	2.30–2.31	2.26–2.28	ADE	7.41
	C _{CO}	1.78–1.81	1.78–1.79	1.79–1.82	λ_{oxi}	0.21
XI	Fe	2.51	2.56	2.57	VDE	0.34
	S ^d	2.28–2.29	2.33–2.34	2.31–2.34	ADE	–0.26
	C _{CO}	1.74–1.75	1.74–1.75	1.76–1.77	λ_{oxi}	0.60
	C _{CO} ^d	–	–	1.83 ^b , 2.23 ^c		
XII	Fe	2.56	2.61	2.61	VDE	6.66
	S ^d	2.25–2.26	2.28–2.29	2.25–2.36	ADE	6.31
	C _{CO}	1.75–1.77	1.76	1.77–1.78	λ_{oxi}	0.35
	P	2.24	2.26	2.29		

^a X-ray values are for Fe(I)–Fe(I) species.

^b Distances from distal iron.

^c Distances from proximal iron.

^d Denotes bridging atom.

lengthening of the Fe–Fe bond by 0.02 Å is found experimentally, a feature which is accurately reproduced by our calculations. It is interesting to note that in common with the enzyme models VI and VII, we find in the case of XI, the formation of a bridging CO in the oxidized species. Our calculated Fe–Fe distance is slightly longer than the X-ray value for X, consistent with other calculations [26].

As far as the ionization energies are concerned, we note that the reorganization energies are generally larger than

for the models (I–V). The magnitude of the ionization energies is mainly dependent on the charges on the species, with the largest values being for the three neutral species (VIII, X and XII) compared to those for the 2-species, IX, XI. In contrast to the two enzyme models, where the ionization energy increases when NH is substituted for CH₂, the ionization energy decreases on going from VIII (CH₂) to X (NCH₃) which may suggest a potential role of the third sulfur atom and cyanides in modulating the ionization energies.

4. Conclusions

We have found that the available structural data does not allow a clear discrimination between the different density functionals and basis sets which can be used to model the iron-only hydrogenases. The ionization energies of model compounds as measured by ESI–PES, might be very useful in this respect and can possibly give some insight into the nature of the bridge-head group and structural changes upon ionization.

References

- [1] M.H. Baik, M. Newcomb, R.A. Friesner, S.J. Lippard, *Chem. Rev.* 103 (2003) 2385.
- [2] E.I. Solomon, *Inorg. Chem.* 40 (2001) 3656.
- [3] X. Amashukeli, N.E. Gruhn, D.L. Lichtenberger, J.R. Winkler, H.B. Gray, *J. Am. Chem. Soc.* 126 (2004) 15566.
- [4] R.A. Marcus, N. Sutin, *Biochim. Biophys. Acta* 811 (1985) 265.
- [5] X.B. Wang, L.S. Wang, *J. Chem. Phys.* 112 (2000) 6959.
- [6] P. Kennopohl, E.I. Solomon, *Inorg. Chem.* 42 (2003) 696.
- [7] L.S. Wang, X.B. Wang, *J. Phys. Chem. A* 104 (2000) 1978.
- [8] P. Kennopohl, E.I. Solomon, *Inorg. Chem.* 42 (2003) 679.
- [9] X.B. Wang, S. Niu, X. Yang, S.K. Ibrahim, C.J. Pickett, T. Ichiye, L.S. Wang, *J. Am. Chem. Soc.* 125 (2003) 14072.
- [10] S. Niu, X.B. Wang, X. Yang, L.S. Wang, T. Ichiye, *J. Phys. Chem. A* 108 (2004) 6750.
- [11] M. Sundararajan, I.H. Hillier, N.A. Burton, *J. Phys. Chem. A* 110 (2006) 785.
- [12] J.W. Tye, M.B. Hall, M.Y. Darensbourg, *Proc. Natl. Acad. Sci.* 102 (2005) 16911.
- [13] Y. Nicolet, C. Piras, P. Legrand, C.E. Hatchikian, J.C. Fontecilla-Camps, *Structure* 7 (1999) 13.
- [14] H.J. Fan, M.B. Hall, *J. Am. Chem. Soc.* 123 (2001) 3828.
- [15] Z. Cao, M.B. Hall, *J. Am. Chem. Soc.* 123 (2001) 3734.
- [16] M. Razavet, S.J. Borg, D.L. Hughes, C.J. Pickett, *Chem. Commun.* (2001) 847.
- [17] M. Razavet, S.J. Borg, S.J. George, S.P. Best, S.A. Fairhurst, C.J. Pickett, *Chem. Commun.* (2002) 700.
- [18] E.J. Lyon, I.P. Georgakaki, J.H. Reibenspies, M.Y. Darensbourg, *Angew. Chem., Int. Ed.* 38 (1999) 3178.
- [19] M. Schmidt, S.M. Contakes, T.B. Rauchfuss, *J. Am. Chem. Soc.* 121 (1999) 9736.
- [20] H. Li, T.B. Rauchfuss, *J. Am. Chem. Soc.* 124 (2002) 726.
- [21] V.E. Kaasjager, R.K. Henderson, E. Bouwmann, M. Lutz, A.L. Spek, J. Reedijk, *Angew. Chem., Int. Ed.* 37 (1998) 1668.
- [22] C. Tard, X. Liu, S.K. Ibrahim, M. Bruschi, L.D. Gioia, S.C. Davies, X. Yang, L.S. Wang, G. Sawers, C.J. Pickett, *Nature* 433 (2005) 610.
- [23] X. Yang, M. Razavet, X.B. Wang, C.J. Pickett, L.S. Wang, *J. Phys. Chem. A* 107 (2003) 4612.
- [24] G. Zampella, M. Bruschi, P. Fantucci, M. Razavet, C.J. Pickett, L. De Gioia, *Chem. Eur. J.* 11 (2005) 509.
- [25] Z.P. Liu, P. Hu, *J. Am. Chem. Soc.* 124 (2002) 5175.
- [26] J.D. Lawrence, H. Li, T.B. Rauchfuss, M. Benard, M.M. Rohmer, *Angew. Chem., Int. Ed.* 40 (2001) 1768.
- [27] X. Zhao, I.P. Georgakaki, M.L. Miller, J.C. Yarbrough, M.Y. Darensbourg, *J. Am. Chem. Soc.* 123 (2001) 9710.
- [28] L. Schwartz, G. Eilers, L. Eriksson, A. Gogoll, R. Lomoth, S. Ott, *Chem. Commun.* 520 (2006).
- [29] A.D. Becke, *Phys. Rev. A* 38 (1988) 3098.
- [30] J.P. Perdew, *Phys. Rev. B* 33 (1986) 8822.
- [31] (a) P.J. Hay, W.R. Wadt, *J. Chem. Phys.* 82 (1985) 299;
(b) M. Couty, M.B. Hall, *J. Comput. Chem.* 17 (1996) 1359;
(c) A.W. Ehlers, M. Bohme, S. Dapprich, A. Gobbi, A. Hollwarth, V. Jonas, K.F. Kohler, R. Stegmann, A. Veldkamp, G. Frenking, *Chem. Phys. Lett.* 208 (1993) 111;
(d) A. Hollwarth, M. Bohme, S. Dapprich, A.W. Ehlers, A. Gobbi, V. Jonas, K.F. Kohler, R. Stegmann, A. Veldkamp, G. Frenking, *Chem. Phys. Lett.* 208 (1993) 237;
(e) T.H. Dunning Jr., P.J. Hay, in: H.F. Schaefer III (Ed.), *Modern Theoretical Chemistry*, vol. 3, Plenum Press, New York, 1976.
- [32] (a) R. Krishnan, J.S. Binkley, R. Seeger, J.A. Pople, *J. Chem. Phys.* 72 (1980) 650;
(b) T. Clark, J. Chandrasekhar, G.W. Spitznagel, P. von R. Schleyer, *J. Comp. Chem.* 4 (1983) 294;
(c) P.M.W. Gill, B.G. Johnson, J.A. Pople, M.J. Frisch, *Chem. Phys. Lett.* 197 (1992) 499;
(d) M.J. Frisch, J.A. Pople, J.S. Binkley, *J. Chem. Phys.* 80 (1984) 3265.
- [33] M.J. Frisch, G.W. Trucks, H.B. Schlegel, G.E. Scuseria, M.A. Robb, J.R. Cheeseman, J.A. Montgomery Jr., T. Vreven, K.N. Kudin, J.C. Burant, J.M. Millam, S.S. Iyengar, J. Tomasi, V. Barone, B. Mennucci, M. Cossi, G. Scalmani, N. Rega, G.A. Petersson, H. Nakatsuji, M. Hada, M. Ehara, K. Toyota, R. Fukuda, J. Hasegawa, M. Ishida, T. Nakajima, Y. Honda, O. Kitao, H. Nakai, M. Klene, X. Li, J.E. Knox, H.P. Hratchian, J.B. Cross, V. Bakken, C. Adamo, J. Jaramillo, R. Gomperts, R.E. Stratmann, O. Yazyev, A.J. Austin, R. Cammi, C. Pomelli, J.W. Ochterski, P.Y. Ayala, K. Morokuma, G.A. Voth, P. Salvador, J.J. Dannenberg, V.G. Zakrzewski, S. Dapprich, A.D. Daniels, M.C. Strain, O. Farkas, D.K. Malick, A.D. Rabuck, K. Raghavachari, J.B. Foresman, J.V. Ortiz, Q. Cui, A.G. Baboul, S. Clifford, J. Cioslowski, B.B. Stefanov, G. Liu, A. Liashenko, P. Piskorz, I. Komaromi, R.L. Martin, D.J. Fox, T. Keith, M.A. Al-Laham, C.Y. Peng, A. Nanayakkara, M. Challacombe, P.M.W. Gill, B. Johnson, W. Chen, M.W. Wong, C. Gonzalez, J.A. Pople, *GAUSSIAN 03 (Revision C.02)*, Gaussian, Inc., Wallingford CT, 2004.
- [34] F.H. Allen, *Acta Crystallogr. B* 58 (2002) 380.